

Analysis of Modular Multilevel Converters with Dc Short Circuit Fault Blocking Capability Bipolar HVDC Transmission Systems

Navitha Petla

M.Tech- EPS,

Department of EEE,

St. Martins Engineering College, Hyd, T.S, India.

T.Achyutha Rao

Professor,

Department of EEE,

St. Martins Engineering College, Hyd, T.S, India.

ABSTRACT:

This project proposes a model predictive control (MPC) method for modular-multilevel-converter (MMC) high-voltage direct current (HVDC). To control the MMC-HVDC system properly, the ac current, circulating current, and submodule (SM) capacitor voltage are taken into consideration. The existing MPC methods for the MMC-HVDC system utilize weighting factors to configure the cost function in combinations of the SM capacitor voltage balancing algorithm, ac current control, and circulating current control. Because all combinations of the switch states are considered in order to minimize the cost function, their possible combinations increase geometrically according to the increase of the level of the MMC, which is a significant disadvantage. This project proposes a new MPC method with a reduced number of states for ac current control, circulating current control, and the SM capacitor voltage-balancing algorithm. The proposed cost functions are divided into three types according to their control purposes. Each cost function determines the minimum number of states for controlling the ac current, circulating current, and SM capacitor voltage. The efficacy of the proposed controlling method is verified through simulation results using MATLAB/Simulink.

INTRODUCTION:

Currently investment and research on high voltage direct current (HVDC) systems have been actively conducted and expanded to improve the efficiency and reliability of electric power generation through large-capacity power transmission and linkage among different networks. Modular multilevel converters seem to have great potential in energy conversion in the near future.

High power applications, such as dc interconnections, dc power grids, and off-shore wind power generation are in need of accurate power flow control and high-efficiency power conversion in order to reduce both their operating costs and their environmental impact.

1) Line-commutated current-source converters (CSCs) that use thyristors (Fig. 1, CSC-HVdc): This technology is well established for high power, typically around 1000 MW, with the largest project being the Itaipu system in Brazil at 6300 MW power level. The longest power transmission in the world will transmit 6400 MW power from the Xiangjiaba hydropower plant to Shanghai.

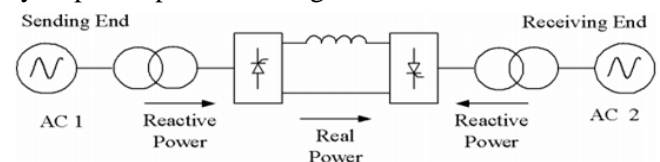


Fig 1: HVDC system based on CSC technology with thyristors

2) Forced-commutated VSCs that use gate turn-off thyristors (GTOs) or in most industrial cases insulated gate bipolar transistors (IGBTs) (Fig. 2, VSC-HVdc): It is well-established technology for medium power levels, thus far, with recent projects ranging around 300–400 MW power level.

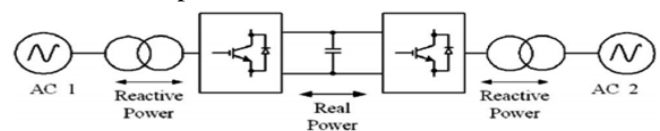


Fig 2: HVDC system based on VSC technology built with IGBTs

On the other hand, VSC-HVdc systems represent recent developments in the area of dc power transmission technology [48].

The experience with VSC-HVdc at commercial level scatters over the last 12 years. The breakthrough was made when the world's first VSC-based PWM-controlled HVdc system using IGBTs was installed in March 1997 (Hellsjon project, Sweden, 3 MW, 10 km distance, " ±10 kV). Elimination of Redundant Voltage Vectors: As presented in Section I, the five-level inverter generates 125 voltage vectors, there are some redundant vectors generated with different voltage levels. With C cells in each leg of the CHB inverter, the amount of non-redundant voltage vectors is $V = 12C^2 + 6C + 1$.

Modular Multilevel Converters

Introduction:

The development of new technologies and devices during the 20th century enhanced the interest in electric power systems. Modern civilization based his operation on an increasing energy demand and on the substitutions of human activities with complex and sophisticated machines; thus, studies on electric power generation and conversion devices become every day more and more important.

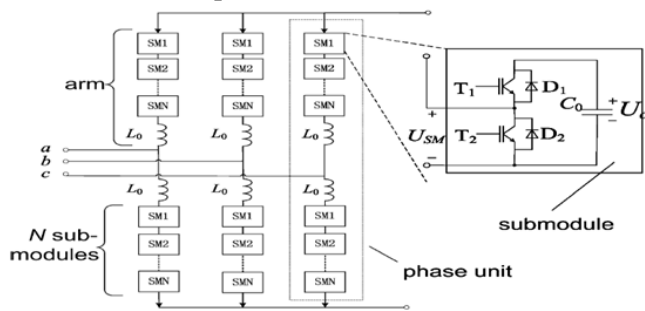


Fig 3: Basic structure of MMC

Description and principle of operation of MMC:

The typical structure of a MMC is shown in Fig. 2, and the configuration of a Sub Module (SM) is given in Fig. 3. Each SM is a simple chopper cell composed of two IGBT switches (T1 and T2), two anti-parallel diodes (D1 and D2) and a capacitor C. Each phase leg of the converter has two arms, each one constituted by a number N of SMs. In each arm there is also a small inductor to compensate for the voltage difference between upper and lower arms produced when a SM is switched in or out.

With reference to the SM shown in Fig. 2, the output voltage U_O is given by,

$$U_O = U_C \text{ if } T1 \text{ is ON and } T2 \text{ is OFF}$$

$$U_O = 0 \text{ if } T1 \text{ is OFF and } T2 \text{ is ON}$$

Where U_C is the instantaneous capacitor voltage

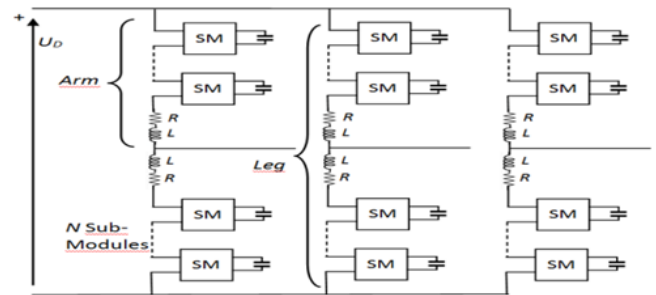


Figure 4: Schematic of a three-phase Modular Multi-level Converter.

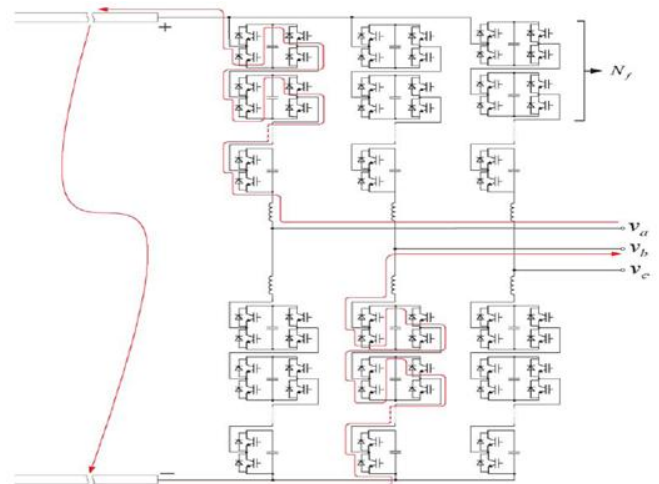


Fig. 5: Block diagram of a hybrid MMC-HVDC system, including the half-bridge and full-bridge SMs with a highlighted dc-fault current path.

SIMULATION RESULTS:

In this section, the performance of various MMCs with different SM configurations is evaluated and compared based on simulation studies conducted on a 21-level MMC-HVDC converter station in the PSCAD/EMTDC environment. The study system parameters are listed in Table III.

A. Case 1: Comparative Studies for Various MMC Configurations

In Table IV, six MMC configurations based on the half-bridge, the full-bridge, the clamp-double, the

unipolar-voltage full-bridge, the three-level cross-connected, and the five-level cross-connected SMs in terms of the semiconductor power losses and the required number of semiconductor component tsare compared. In normal operating mode, the MMC system of Fig. 1 is in a steady-state condition and 25-MW real power flows from the dc side to the ac side. The system also provides 18-MVar reactive power.

TABLE IV: COMPARISON OF THE MMC CONFIGURATIONS WITH VARIOUS SMS

MMC configuration	Half-bridge MMC	Full-bridge MMC	Clamp-double MMC	Unipolar-voltage full-bridge MMC	Three-level cross-connected MMC	Five-level cross-connected MMC
SM circuit	HBSM	FBSM	CDSM	UFBSM	3LCCSM	5LCCSM
Dc-fault-handling capability	×	✓	✓	✓	✓	✓
Voltage levels	21	21	21	21	21	21
No. of capacitors per arm	20	20	20	20	20	20
No. of SMs per arm	20	20	10	20	10	10
No. of IGBTs/diodes per arm (inserting/bypassing SMs)	40	80	40	40	40	40
No. of extra switches per arm (conducting switches)	0	0	10 (S5)	20 (S4)	20 (S5)	40 (S5, S6)
No. of extra diodes per arm	0	0	20 (D6, D7)	20 (D3)	20 (D6)	0
Estimated power loss	0.09%	0.96%	0.83%	0.96%	0.83%	0.83%
Extra power loss compared to the half-bridge MMC	0	38%	19%	38%	38%	38%

TABLE V: COMPARISON OF THE HYBRID MMC CONFIGURATIONS WITH VARIOUS SMS

MMC configuration	Hybrid design I	Hybrid design II	Hybrid design III	Hybrid design IV	Hybrid design V
SM circuit	HBSM-FBSM	HBSM-CDSM	HBSM-UFBSM	HBSM-3LCCSM	HBSM-5LCCSM
Dc-fault-handling capability	✓	✓	✓	✓	✓
Voltage levels	21	21	21	21	21
No. of capacitors per arm	20	20	20	20	20
No. of SMs per arm	20	12	20	16	16
No. of HBSM per arm	12	4	12	12	12
No. of FBSM per arm	8	0	0	0	0
No. of CDSM per arm	0	8	0	0	0
No. of UFBSM per arm	0	0	8	0	0
No. of 3LCCSM per arm	0	0	0	4	0
No. of 5LCCSM per arm	0	0	0	0	4
No. of IGBTs/diodes per arm (inserting/bypassing SMs)	56	40	40	40	40
No. of extra switches per arm (conducting switches)	0	8 (S5)	8 (S4)	16 (S5, S6)	8 (S5)
No. of extra diodes per arm	0	16 (D6, D7)	8 (D3)	0	8 (D6)
Estimated power loss	0.798%	0.798%	0.798%	0.798%	0.798%
Extra power loss compared to the half-bridge MMC	16%	16%	16%	16%	16%

Case 2: DC-Side Fault Handling Based on Hybrid Design III and V:

In this section, the dc-fault-handling capability of the hybrid designed MMC systems is demonstrated. Figure 7 shows the study results of the hybrid design III. Initially, the system of Fig. 1 is in a steady-state condition, that is, P=25 MW and Q=18 MVar. At 0.5 s, a dc-side short-circuit fault occurs, lasting for 100 ms. The fault is cleared at t=0.7 s when the MMC system is recovered to transfer power.

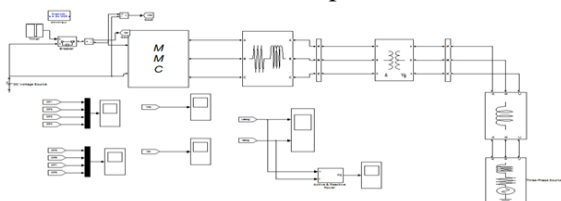


Fig 6: Simulation circuit of the proposed MMC converter

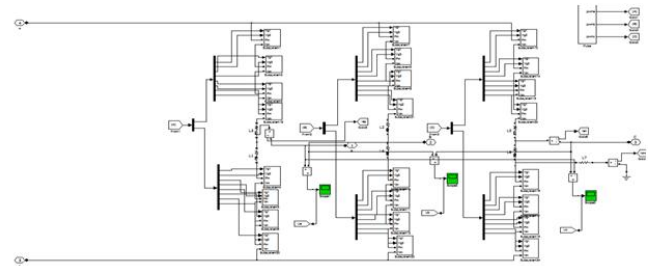
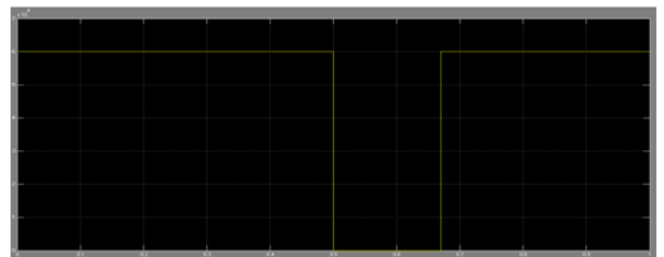
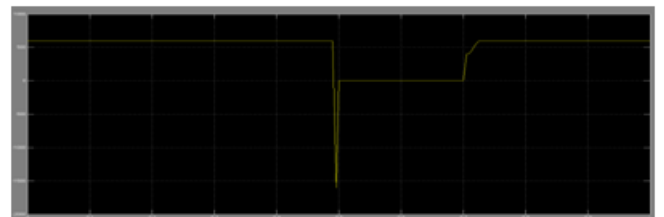


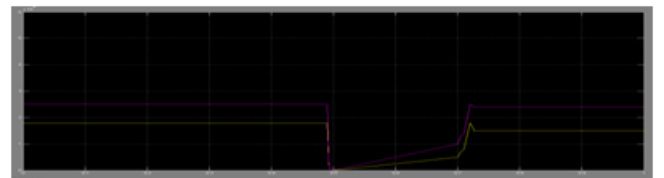
Fig 6: Internal Design of the MMC



(a)



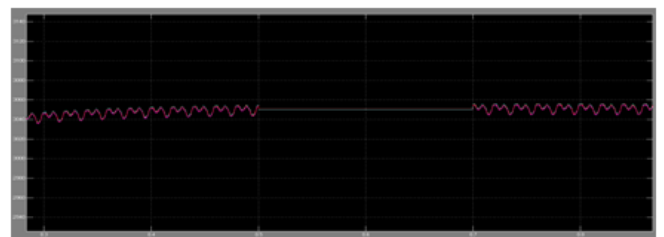
(b)



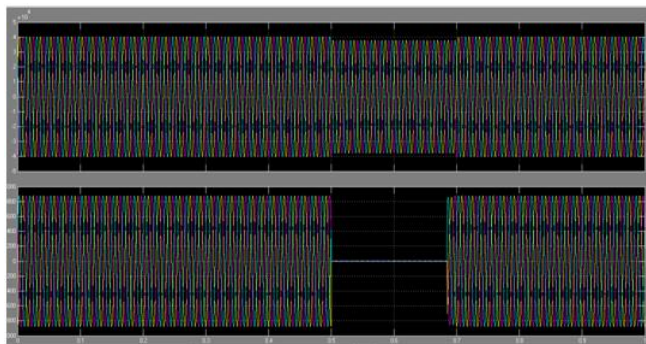
(c)



(d)



(e)



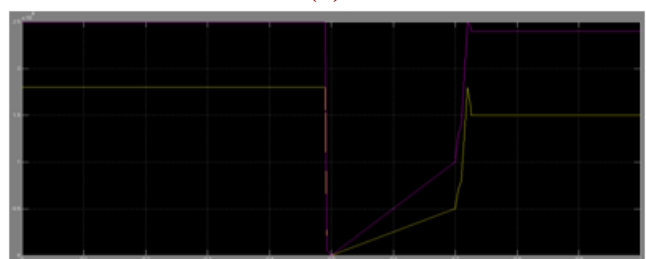
(f& g) Fig. 7. DC-side short-circuit fault handling of the hybrid-designed MMCHVDC system (hybrid design III) with the half-bridge and unipolar-voltage full-bridge SMs: (a) and (b) dc voltage and current, (c) real and reactive power, (d) and (e) SM capacitor voltages of the upper and lower arms of phase- , (f), and (g) ac-side currents and voltages.



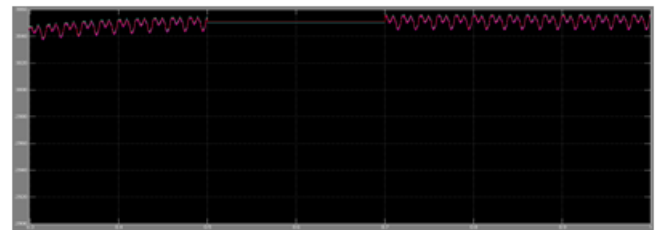
(a)



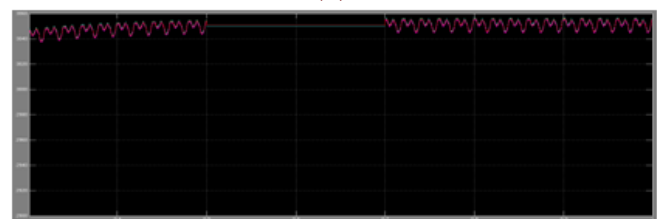
(b)



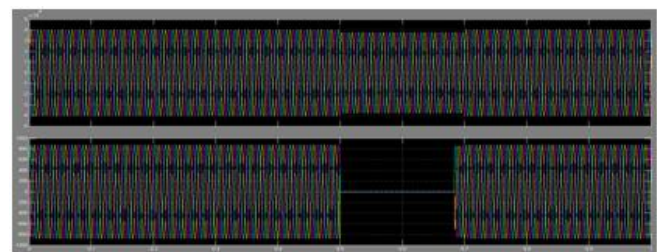
(c)



(d)



(e)



(f& g) Fig. 8: DC-side short-circuit fault handling of the hybrid-designed MMCHVDCsystem (hybrid design V) with the half-bridge and three-level cross-connectedSMs: (a) and (b) dc voltage and current, (c) real and reactive power, (d) and (e) SM capacitor voltages of the upper and lower arms of phase- , (f), and (g) ac-side currents and voltages.

THE PROPOSED METHOD FOR MMC-HVDC SYSTEM

A. Multiloop control strategy:

The MMC converter consists of three independent H-bridges that are connected to a common dc-link capacitor. VSCs are connected in series to the supply grid through a single phase transformer. The proposed Fault Current Interruption (FCI) consists of independent and identical controllers for single phase VSC of the MMC. The fundamental frequency components of supply voltage V_s , load voltage V_l and injected voltage V_{inj} .

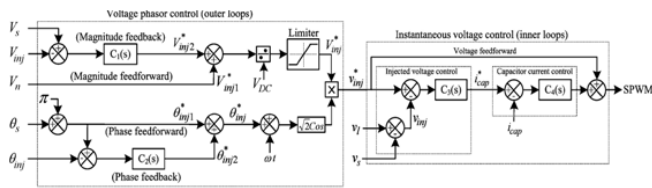


Fig 9: Block diagram of multi loop control strategy

$$v_s = V_s \times \cos(\omega t + \theta_s) \quad (1)$$

$$v_1 = V_1 \times \cos(\omega t + \theta_1) \quad (2)$$

$$v_s = v_s - v_1 = V_{inj} \times \cos(\omega t + \theta_{inj}) \quad (3)$$

The FCI function requires a phasor parameter estimator (digital filter) which attenuates the harmonic contents of the measured signal. To attenuate all harmonics, the filter must have a full-cycle data window length which leads to one cycle delay in the MMC response. Thus, a compromise between the voltage injection speed and disturbance attenuation is made. FCI performs satisfactorily under fault conditions where the measured voltages and current signals are highly distorted. Fig. 9 shows a per-phase block diagram of the proposed MMC control system corresponding to the FCI operation mode, where V_n is the nominal rms phase voltage. The control system of Fig. 9 utilizes the dc-link voltage VDC and the harmonic filter capacitor current i_{cap} as the input signals.

The study in this paper is based on the fault current detection method. The fault detection mechanism for each phase is activated when the absolute value of the instantaneous current exceeds twice the rated load current. The proposed multiloop control system includes an outer control loop (voltage phasor control) and an inner control loop (instantaneous voltage control). The inner loop provides damping for the transients caused by the MMC, and improves the dynamic response and stability of the MMC. When a downstream fault is detected, the outer loop controls the injected voltage magnitude and phase angle of the faulty phase(s) and reduces the load-side voltage to zero, to interrupt the fault current and restore the PCC voltage.

VOLTAGE PHASOR CONTROL:

In the FCI operation mode, the required injected voltage phasor is equal to the source voltage phasor. Performance of the voltage phasor control, in terms of transient response, speed, and steady-state error, is enhanced by independent control of voltage magnitude and phase, and incorporating feed forward signals to the feedback control system. Parameters of each controller are determined to achieve a fast response with zero steady-state error. The output of the phasor control system is a reference phasor denoted by

$$V_{inj}^* = V_{inj}^* \times \theta_{inj}$$

To eliminate the effects of the dc-link voltage variations on the injected voltages, V_{inj}^* is normalized by VDC.

C. INSTANTANEOUS VOLTAGE CONTROL:

Under ideal conditions, a voltage sag can be effectively compensated if the output of the phasor-based controller is directly fed to the sinusoidal pulse-width modulation (SPWM) unit. However, resonances of the harmonic filter cannot be eliminated under such conditions. Therefore, to improve the stability and dynamic response of the MMC, an instantaneous injected voltage controller and a harmonic filter capacitor current controller are used to attenuate resonances. The generated reference signal for the injected voltage V_{inj}^* is compared with the measured injected voltage V_{inj} , and the error is fed to the voltage controller. The output of the voltage controller i_{cap}^* is the reference signal for the filter capacitor current control loop. The steady-state error of the proposed control system is fully eliminated by the PI controllers in the outer control loop (i.e. C1 and C2) which track dc signals (magnitude and phase angle). Therefore, there is no need for higher order controllers in the inner control loop which are designed based on sinusoidal references. A large result in amplification of the MMC. Filter resonance and can adversely impact the system stability [18].

Thus, the transient response of the MMC is enhanced by a feed forward loop, and a small proportional gain

is utilized as the voltage controller. A large damps the harmonic filter resonance more effectively, but it is limited by practical considerations (e.g., amplification of capacitor current noise, measurement noise, and dc offset [18]). Therefore, the lowest value of the proportional gain which can effectively damp the resonances is utilized. The output of the current controller is added to the feed forward voltage to derive the signal for the PWM generator. The proposed FCI method limits the maximum fault current to about 2.5 times the nominal value of the load current and interrupts the fault currents in less than 2 cycles. Depicts variations of the dc-link voltage during the FCI operation, and indicates that the dc-link voltage rise under the worst case (i.e., a severe three phase fault).

MATLAB/SIMULINK

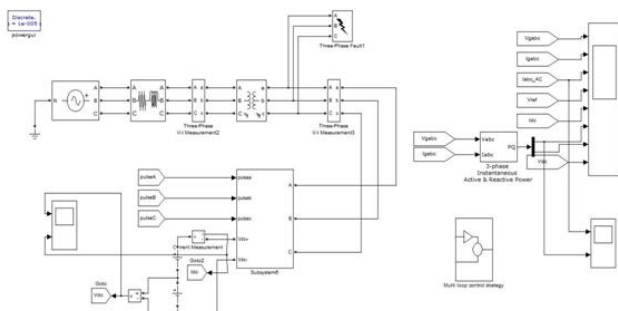


FIG 10: SIMULINK MODEL OF THE PROPOSED SYSTEM

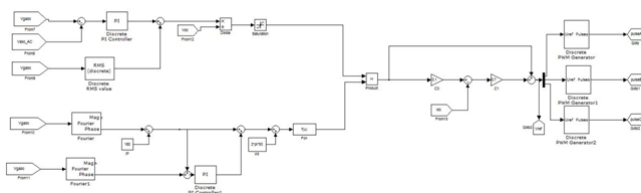


FIG 11: SIMULINK MODEL OF MULTILoop CONTROL

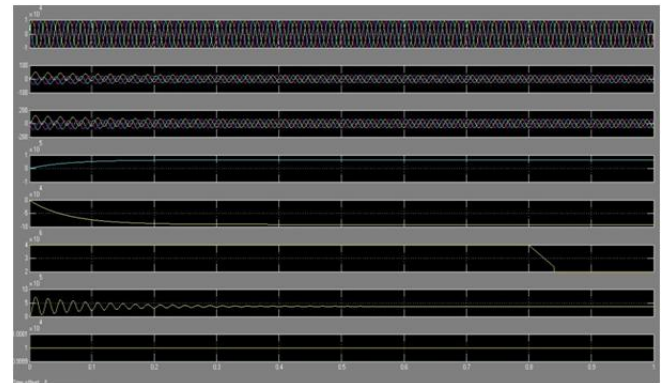


FIG 12: SIMULATION RESULTS UNDER UNBALANCED GRID CONDITIONS: A) GRID CURRENT B) GRID VOLTAGE C) ACTIVE POWER D) REACTIVE POWER E) REFERENCE VOLTAGE F) DC LINK CURRENT G) DC LINK VOLTAGE



FIG 13: SIMULATED OUTPUTS OF DC VOLTAGE AND DC CURRENT

CONCLUSION:

This paper proposes the MPC method with a reduced number of considered states for the MMC-HVDC system. To control the MMC, three cost functions were adopted: first, a cost function to control ac-side current; second, a cost function to control the inner unbalanced current and DC-link current; and third, a cost function for SM capacitor voltage balancing and switch frequency reduction. The proposed MPC method minimizes the number of statuses to be considered by means of the cost functions with the MMC stably controlled. The study results demonstrate that the hybrid-designed MMC configurations based on a combination of the half-bridge and the proposed SM circuits are the optimal design among all evaluated systems in terms of dc fault-handling capability, semiconductor power losses, and semiconductor device requirements.

FUTURE SCOPE:

The Alternate Arm Modular Multilevel Converter is further implemented over Modular multilevel converter topology for VSC based HVDC applications. The major concern of sequential proper switching of capacitors of each sub module can be solved by sorting technique.

REFERENCES:

- [1] S. Debnath, J. Qin, B. Bahrani, M. Saeedifard, and P. Barbosa, "Operation, control, and applications of the modular multilevel converter: A review," *IEEE Trans. Power Electron.*, vol. 30, no. 1, pp. 37–53, Jan. 2015.
- [2] S. Allebrod, R. Hamerski, and R. Marquardt, "New transformerless, scalable modular multilevel converters for HVDC-transmission," in *Proc. IEEE Power Electronics Specialists Conf.*, Jun. 2008, pp. 174–179.
- [3] J. Dorn, H. Huang, and D. Retzmann, "A new multilevel voltage sourced converter topology for HVDC applications," presented at the CIGRE Session, Paris, France, 2008, B4-30.
- [4] R. Marquardt, "Modular multilevel converter: A universal concept for HVDC-networks and extended DC-bus-applications," in *Proc. Int. Power Electron. Conf.*, Jun. 2010, pp. 502–507.
- [5] B. Gemmell, J. Dorn, D. Retzmann, and D. Soerangr, "Prospects of multilevel VSC technologies for power transmission," in *Proc. IEEE Transm. Distrib. Conf. Expo.*, Apr. 2008, pp. 1–16.
- [6] K. Friedrich, "Modern HVDC PLUS application of VSC in modular multilevel converter topology," in *Proc. IEEE Int. Symp. Ind. Electron.*, 2010, pp. 3807–3810.
- [7] M. Saeedifard and R. Iravani, "Dynamic performance of a modular multilevel back-to-back HVDC system," *IEEE Trans. Power Del.*, vol. 25, no. 4, pp. 2903–2912, Oct. 2010.
- [8] J. Peralta, H. Saad, S. Denneriere, J. Mahseredjian, and S. Nguefeu, "Detailed and averaged models for a 401-level MMC-HVDC system," *IEEE Trans. Power Del.*, vol. 27, no. 3, pp. 1501–1508, Jul. 2012.
- [9] J. Qin and M. Saeedifard, "Predictive control of a modular multilevel converter for a back-to-back HVDC system," *IEEE Trans. Power Del.*, vol. 27, no. 3, pp. 1538–1547, Jul. 2012.
- [10] G. T. Son, H.-J. Lee, T. S. Nam, Y.-H. Chug, and U.-H. Lee, "Design and control of a modular multilevel HVDC converter with redundant power modules for noninterruptible energy transfer," *IEEE Trans. Power Del.*, vol. 27, no. 3, pp. 1611–1619, Jul. 2012.
- [11] A. Nami, J. Liang, F. Dijkhuizen, and G. Demetriades, "Modular multilevel converters for HVDC applications: Review on converter cells and functionalities," *IEEE Trans. Power Electron.*, vol. 30, no. 1, pp. 18–36, Jan. 2015.
- [12] L. Tang and B.-T. Ooi, "Locating and isolating dc faults in multiterminal dc systems," *IEEE Trans. Power Del.*, vol. 22, no. 3, pp. 1877–1884, Jul. 2007.